International Journal of Pharmaceutics: X 8 (2024) 100268

Contents lists available at ScienceDirect

International Journal of Pharmaceutics: X

journal homepage: www.sciencedirect.com/journal/international-journal-of-pharmaceutics-x

Enhancing oocyte in vitro maturation and quality by melatonin/bilirubin cationic nanoparticles: A promising strategy for assisted reproduction techniques

Haitao Xi [a,b,c,1], Lihui Huang [a,c,1], Lin Qiu [a,b,1], Shize Li [a,c,d], Yuqi Yan [a,c], Yang Ding [a], Yuhao Zhu [a], Fugen Wu [e], Xianbao Shi [f], Junzhao Zhao [b,c], Ruijie Chen [a,c], Qing Yao [a,d,*], Longfa Kou [a,c,*]

[a] Wenzhou Municipal Key Laboratory of Pediatric Pharmacy, Department of Pharmacy, The Second Affiliated Hospital and Yuying Children's Hospital of Wenzhou Medical University, Wenzhou 325027, China
[b] Reproductive Medicine Center, Department of Obstetrics and Gynecology, The Second Affiliated Hospital and Yuying Children's Hospital of Wenzhou Medical University, Wenzhou 325027, China
[c] Key Laboratory of Structural Malformations in Children of Zhejiang Province, Wenzhou 325027, China
[d] School of Pharmaceutical Sciences, Wenzhou Medical University, Wenzhou 325035, China
[e] Department of Pediatric, The First People's Hospital of Wenling, Taizhou, China
[f] Department of Pharmacy, The First Affiliated Hospital of Jinzhou Medical University, Jinzhou, China

ARTICLE INFO

Keywords:
Oocytes
In vitro maturation
Reactive oxygen species
Melatonin
Bilirubin
Cationic nanoparticles

ABSTRACT

In assisted reproduction techniques, oocytes encounter elevated levels of reactive oxygen species (ROS) during in vitro maturation (IVM). Oxidative stress adversely affects oocyte quality, hampering their maturation, growth, and subsequent development. Thus, mitigating excessive ROS to safeguard less viable oocytes during IVM stands as a viable strategy. Numerous antioxidants have been explored for oocyte IVM, yielding considerable effects; however, several aspects, including solubility, stability, and safety, demand attention and resolution. In this study, we developed nanoparticles by self-assembling endogenous bilirubin and melatonin hormone coated with bilirubin-conjugated glycol chitosan (MB@GBn) to alleviate oxidative stress and enhance oocyte maturation. The optimized MB@GBn exhibited a uniform spherical shape, measuring 128 nm in particle size, with a PDI value of 0.1807 and a surface potential of +11.35 mV. The positively charged potential facilitated nanoparticle adherence to the oocyte surface through electrostatic interaction, allowing for functional action. In vitro studies demonstrated that MB@GB significantly enhanced the maturation of compromised oocytes. Further investigation revealed MB@GB's effectiveness in scavenging ROS, reducing intracellular calcium levels, and suppressing mitochondrial polarization. This study not only offers a novel perspective on nano drug delivery systems for biomedical applications but also presents an innovative strategy for enhancing oocyte IVM.

1. Introduction

Infertility is defined as the inability to achieve a clinical pregnancy without contraception for over a year (Agarwal et al., 2014), affecting both males and females. Ovulatory dysfunction and anovulation play crucial roles in female factor infertility (Carson and Kallen, 2021). Globally, one in six individuals grapple with infertility. Assisted reproductive technology (ART) stands as a pivotal biomedical intervention offering practical and safe solutions to aid infertile couples or individuals in achieving pregnancy. ART comprises in vitro fertilization (IVF) and Intracytoplasmic sperm injection (ICSI) (Njagi et al., 2023). Both methods involve a significant process known as in vitro maturation (IVM), which refers to the cultivation of cumulus-enclosed oocytes retrieved at the GV stage in a nurturing medium to support their developmental potential (De Vos et al., 2021; De Vos et al., 2016). This technique allows the harvesting of immature oocytes, fostering their

* Corresponding authors at: Wenzhou Municipal Key Laboratory of Pediatric Pharmacy, Department of Pharmacy, The Second Affiliated Hospital and Yuying Children's Hospital of Wenzhou Medical University, Wenzhou 325027, China.
E-mail addresses: yqpharm@163.com (Q. Yao), klfpharm@163.com (L. Kou).
[1] The authors contributed equally.

https://doi.org/10.1016/j.ijpx.2024.100268
Received 18 January 2024; Received in revised form 31 May 2024; Accepted 1 July 2024
Available online 2 July 2024

maturation within a laboratory setting (Chian et al., 2013). However, the clinical utilization of IVM has been persistently restricted due to the challenges of low maturity rates and the asynchrony between nuclear and cytoplasmic development (Brown et al., 2017). These issues lead to embryo developmental blocks and a decreased pregnancy rate. IVM oocytes exhibit lower developmental potential compared to naturally matured oocytes (De Vos et al., 2021). Numerous evidence suggests that IVM not only impacts the timing of implantation but also leaves a lasting influence on the health of future generations. Hence, novel methodologies are imperative to enhance the quality of IVM oocytes, thereby refining the effectiveness of IVF and ICSI techniques.

From their release from the ovary to their capture by the fallopian tubes, oocytes await fertilization by a single sperm, typically within a 24-h timeframe (Duffy et al., 2019). The quality of oocyte maturation significantly influences subsequent successful fertilization and early embryo development, playing a pivotal role in animal fertility (Campos et al., 2023). Unlike the female reproductive tract, which maintains a low oxygen concentration (ranging between 2% and 8%), laboratory environments exhibit higher oxygen conditions (Fischer and Bavister, 1993). Many studies have indicated that oocytes undergoing in vitro maturation (IVM) encounter hindered development due to the accumulation of excessive reactive oxygen species (ROS) and the absence of free radical scavengers. Elevated ROS levels in IVM oocytes can lead to cytoplasmic fragmentation, apoptosis, and chemical reactions with biomolecules like lipids and nucleic acids. This interaction may cause genetic material damage and oxidative stress, resulting in failed fertilization. However, oocytes lack the comprehensive ability to activate all antioxidant defense mechanisms (von Mengden et al., 2020). Thus, managing ROS levels in IVM emerges as a promising strategy to enhance oocyte quality. Research indicates that incorporating free radical scavengers into the medium during IVF may foster oocyte maturation, thereby enhancing the prospects of a successful pregnancy (Sugino, 2005; Ng et al., 2018).

Melatonin (MT), a naturally occurring hormone in the human body, serves a pivotal role in various physiological functions encompassing sleep regulation, thermoregulation, metabolism, circadian rhythm, and reproductive physiology (Cipolla-Neto and Amaral, 2018). The presence and levels of melatonin in follicular fluid exhibit a positive correlation with oocyte quality and maturation. Moreover, melatonin and its metabolites possess robust free radical scavenging capabilities (Reiter et al., 2016). Previous research indicates that MT and its metabolites function as direct scavengers and indirect antioxidants of free radicals by modulating the gene expression of antioxidant enzymes like catalase, glutathione peroxidase, and superoxide dismutase (Succu et al., 2014; Liang et al., 2017; Ortiz et al., 2011). Melatonin supplementation during in vitro maturation (IVM) has demonstrated the ability to enhance oocyte maturation in mice, sheep, cattle, and pigs, significantly improving early embryonic development (Ishizuka et al., 2000; Abecia et al., 2002; Papis et al., 2007; Rodriguez-Osorio et al., 2007; Choi et al., 2008). Bilirubin, an endogenous metabolite of heme breakdown, exhibits exceptional antioxidative, anti-inflammatory, immune-modulatory, and cytoprotective properties (Yao et al., 2020a; Yao et al., 2020b; Yao et al., 2020c; Huang et al., 2021; Zhao et al., 2021; Jiang et al., 2022; Jiang et al., 2023; Yao et al., 2023a; Kou et al., 2022a; Huang et al., 2024). Bilirubin alleviates oxidative stress by directly scavenging reactive oxygen species (ROS) or inducing the antioxidative systems, including HO-1, Nrf-2, and GPX4 (Yao et al., 2019a; Yao et al., 2020d; Yao et al., 2019b; Yao et al., 2021; Zhao et al., 2024; Xia et al., 2024). Additionally, the metabolic cycle of bilirubin/biliverdin further enhances its antioxidative properties. However, both compounds are insoluble and susceptible to local oxygen levels, limiting their application in oocyte IVM.

Based on these facts and our prior investigations, we endeavored to create a nanoparticle formulation by directly combining bilirubin and melatonin. This aimed to enhance the solubility of these compounds by nano-sized delivery systems for potential application in oocyte in vitro maturation (IVM) (Xu et al., 2024; Shen et al., 2024; Li et al., 2024). However, the resulting nanoparticles exhibited instability during storage. To address this, we further coated the nanoparticles using a *graft*-modified natural polymer known as bilirubin-conjugated glycol chitosan. The grafting of bilirubin bolstered the polymer coating's adhesion to the nanoparticles through a matching effect. This polymer coating not only significantly improved the stability of the nanoparticles but also conferred a positive potential, facilitating their adherence to oocytes for immediate protection. The optimized formulation, bilirubin-conjugated glycol chitosan-coated bilirubin/melatonin nanoparticles (MB@GBn), displayed notable efficacy in safeguarding and promoting the maturation of substandard oocytes (Fig. 1). These results highlight the considerable potential of MB@GB for use in oocyte IVM applications. Our study offers a fresh perspective on the utilization of nanomedicine and addresses pertinent clinical challenges in this domain.

2. Materials and methods

2.1. Materials

Bilirubin, Coumarin 6 (C6) and glycol chitosan were procured from Macklin Biochemical Co., Ltd. (Shanghai, China). Melatonin, N-(3-Dimethylaminopropyl)-N′-ethylcarbodiimide hydrochloride (EDC), and N-Hydroxysuccinimide (NHS) were sourced from Aladdin Biochemical Co., Ltd. (Shanghai, China). The ROS assay kit, Fluo-4 Calcium Assay Kit were purchased from Beyotime Biotechnology Co. Ltd. (Shanghai, China). The Mitochondrial membrane potential assay kit was acquired from Abbkine Scientific Co., China. Bovine serum albumin (BSA) was obtained from Solarbio Science and Technology (Beijing, China). Bovine serum albumin (BSA) for oocytes, Medium199, and Dulbecco's modified eagle medium (DMEM) were obtained from Gibco (Massachusetts, USA). Cell culture dishes/plates and centrifuge tubes were procured from NEST Biotechnology Co., Ltd. (Wuxi, China). All other chemicals or solvents are of analytical grade.

2.2. Synthesis and characterization of bilirubin grafted glycol chitosan (GC-BR)

The synthesis of the glycol chitosan-bilirubin conjugate (GC-BR) involved coupling the carboxyl group of bilirubin with the amino group of glycol chitosan. Initially, bilirubin, NHS, and EDC were added to dimethyl sulfoxide (DMSO) and stirred at room temperature for 1 h. Subsequently, glycol chitosan was introduced into the mixed solution, and the stirring continued for 24 h. The resulting mixture was then dialyzed in distilled water for an additional 24 h to remove unconjugated BR and residual chemicals. Post-lyophilization, the final product, GC-BR, was obtained. Characterization of the synthesized GC-BR was performed using ^{1}H nuclear magnetic resonance (^{1}H NMR) and Fourier transform infrared (FTIR) techniques.

2.3. Preparation of glycol chitosan bilirubin conjugate-coated bilirubin/melatonin nanoparticles (MB@GBn)

The process for preparing melatonin-loaded nanoparticles involved a modified nanoprecipitation method. Initially, bilirubin and melatonin were dissolved separately in DMSO and then combined at a molar ratio of 1:5. Subsequently, GC-BR, constituting 20% of the total mass of bilirubin and melatonin, was added to the mixture and vortexed for approximately 30 s. Once evenly mixed, the solution was slowly dropped into double-distilled water being stirred at a ratio of 1:10 (*v*/v) on a magnetic stirrer (200 rpm) to yield the nanoparticle solution. The resulting solution was then dialyzed in distilled water for 2 h to remove the organic solvent and residual compounds. Post-lyophilization, the final nanoparticles, MB@GBn, was obtained. Coumarin 6 (C6) was selected to monitor the intracellular behavior of MB@GBn. The C6-loaded MB@GBn was prepared by a similar method described above

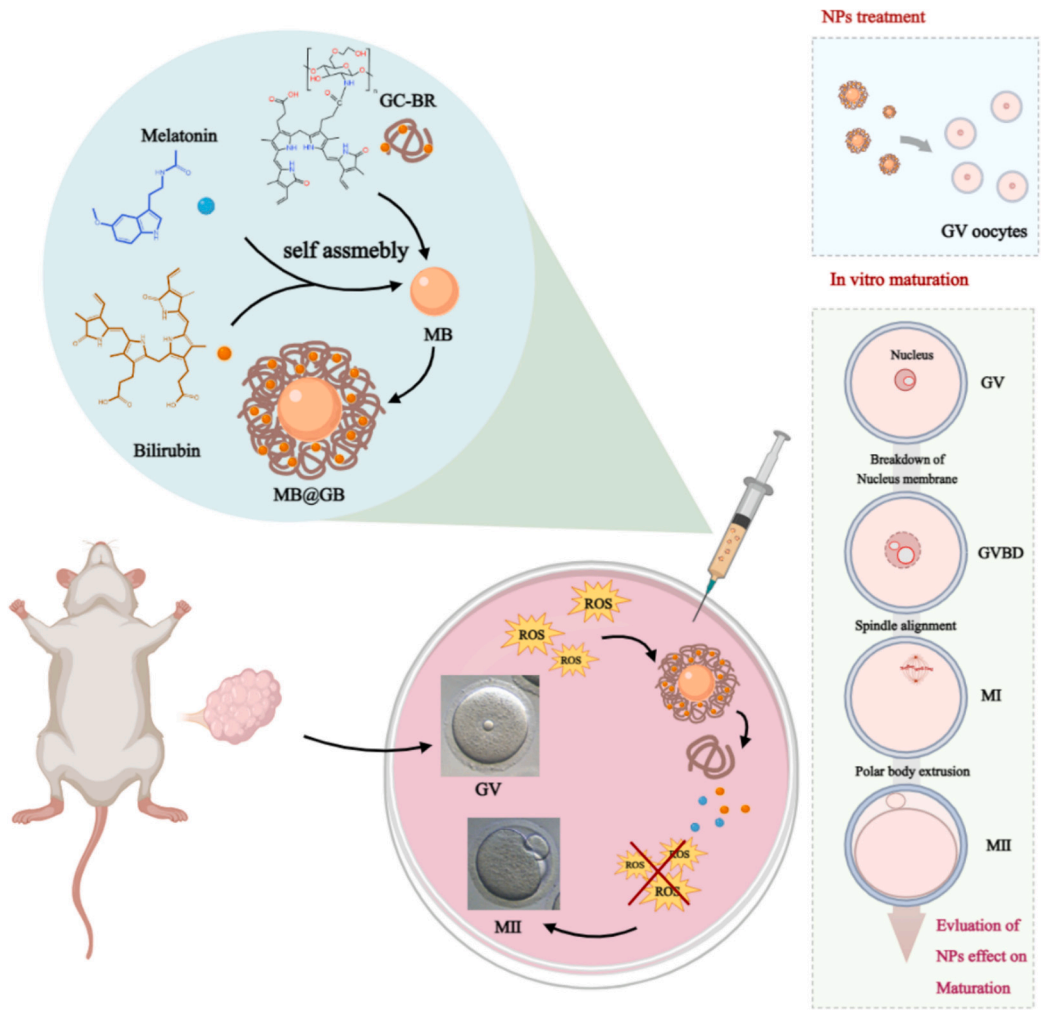

Fig. 1. Schematic diagram for the preparation of MB@GBn and its application for enhancing IVM. MB@GBn could bind to oocyte surface by mild electrostatic force, and then display notable efficacy in safeguarding and promoting the maturation of substandard oocytes by scavenging ROS, regulating intracellular Ca^{2+}, and modulating mitochondrial membrane potential.

except adding C6 (the molar ratio of C6:BR was 1:10) into the mixture before GC-BR addition.

2.4. Characterization of MB@GBn

The prepared MB@GBn were characterized for evaluation and optimization. The particle size, size distribution, and zeta potential of MB@GBn were determined by NanoZetasizer (MALVERN Zetasizer Nano ZS). The morphology of MB@GBn was observed using transmission electron microscopy (TEM) with the JEM 1200EX instrument (JEOL Ltd., Tokyo, Japan).

The encapsulation efficiency (EE) and drug load (DL) of melatonin in MB@GBn was measured using HPLC, which was equipped with a Zorbax Eclipse XDB C18 column (5 μm, 4.6 × 150 mm, Agilent, USA) at a constant temperature of 25 °C and detection at a wavelength of 230 nm. The mobile phase was a mixture of methanol and water (55/45, *v*/v) at a flow rate of 0.8 mL/min. EE and DL were calculated using the following formulas.

EE (%) = (weight of encapsulated drugs/weight of added drug) × 100%.

DL (%) = (weight of encapsulated drugs/weight of total nanoparticles) × 100%.

The release profiles of melatonin (MT) from the nanoparticles were determined via a modified dialysis method (Kou et al., 2022b; Chen et al., 2022a; Yao et al., 2024; Chen et al., 2024; Yao et al., 2023b). Briefly, 1 mL of free MT or MT-loaded nanoparticles was incubated in a dialysis bag (MWCO: 3000 Da) placed in 30 mL of pH 7.4 PBS containing 0.1% sodium dodecyl sulfate (SDS) at 37 °C and 100 rpm. Samples were collected at specific intervals, and concentration determination was performed using HPLC after filtration through a 0.22-μm filter. Additionally, the release assays were conducted in an environment enriched with 0.3% H_2O_2 (*v*/v) to simulate a ROS-rich condition.

For stability assay, the nanoparticles were dispersed in distilled water, and their size and Polydispersity Index (PDI) were measured using NanoZetasize at 4 °C. Concurrently, to test ROS-response characteristics, the nanoparticles were dispersed in double-distilled water containing 0.3% H_2O_2. Measurements of particle size and PDI were taken at 0, 10, 30, and 60 min, and morphological changes were observed via TEM.

2.5. Cell line and animals

The Human Umbilical Vein Endothelial Cells (HUVEC) were sourced from the Cell Bank of the Type Culture Collection of the Chinese Academy of Sciences (Shanghai, China). The HUVEC cells were cultivated in Dulbecco's Modified Eagle's Medium (DMEM), supplemented with 10% Fetal Bovine Serum (FBS), 50 units/mL of streptomycin, and 100 units/mL of penicillin. These cells were maintained in an incubator at 37 °C with 5% CO_2.

Female Institute of Cancer Research (ICR) mice aged 4 weeks were

procured from Wenzhou Medical University Experimental Animal Center and were housed under specific pathogen-free (SPF) conditions. All animal-related procedures adhered to the regulations outlined by the Wenzhou Medical University Experimental Animal Center and were approved by the Experimental Animal Ethics Committee of Wenzhou Medical University (wydw2021–0333).

2.6. Collection and treatment of mouse oocytes

Ovaries were harvested from 4-week-old female ICR mice approximately 46–48 h post intraperitoneal injection of 10 IU pregnant mare serum gonadotropin (NSHF, Ningbo, China). Using a 1 mL syringe equipped with a 26-gauge needle, germinal vesicle (GV)-stage oocytes were extracted by puncturing the ovaries. Following extraction, the oocytes were segregated into two groups: the control group (IOs, COCs) and the experimental group. The cumulus cell layer surrounding the oocytes was removed using fine glass capillaries in all groups, excluding the COCs group. Various concentrations of MB@GBn (0.5, 1, 2.5×10^{-5} M, equivalent to the concentration of MT in MB@GBn) were introduced into the medium of the experimental group and incubated for approximately 16 h. Post-treatment, the samples were prepared for subsequent experiments.

2.7. Cellular uptake assay

Cellular uptake was performed to investigate the behavior of MB@GBn when incubated with HUVEC cells or mouse oocytes. Briefly, HUVEC cells were seeded in 12-well plate containing cover slips with a concentration of 1.0×10^5 cells/well. After 12 h for cell adherence, the cells were treated with Coumarin 6 (C6)-loaded MB@GBn (4 μg/mL of C6) with difference time. Following that, the cells were washed with cold PBS for three times, and the cover slips were collected and placed onto the glass slides with a drop of mountant containing DAPI. Afte 1 h, the slides could be observed under a fluorescence microscope. The fluorescence was quantified by Image J software.

For the uptake of MG@GBn in mouse oocytes, the procedure was similar. Oocytes were dispersed in culture media, and the Coumarin 6 (C6)-loaded MB@GBn (4 μg/mL of C6) was added into the media for incubation. After certain times, the oocytes were collected and visualized under a fluorescence microscope. The fluorescence was quantified by Image J software.

2.8. In vitro maturation

The oocytes from each group grow in M199 medium (Gibco, USA) supplemented with 0.1 mM sodium pyruvate, 75 mIU/mL FSH, 10% bovine serum albumin (Gibco, USA) and 1% penicillin-streptomycin and incubated in a humidified 5% CO_2 incubator at 37 °C for approximately 16 h. During this period, germinal vesicle (GV)-stage oocytes progress through germinal vesicle breakdown (GVBD), metaphase of meiosis I (MI), and reach the metaphase II (MII) stages. The maturation ratio was determined by calculating the proportion of mature oocytes to the total number of oocytes.

2.9. Mitochondrial membrane potential (MMP) detection in oocytes

The mitochondrial membrane potential (MMP) of the oocytes was assessed using the Mitochondrial Membrane Potential Assay Kit (Abbkine Scientific Co., China). In brief, mouse oocytes were exposed to 10 μM JC-1 in 100 μL of working solution at 37 °C for 30 min, followed by three washes with PBS. Subsequently, the fluorescence intensity was visualized under a fluorescence microscope (LSM 800, Zeiss, Germany). The MMP was quantified as the ratio of red fluorescence (indicating activated mitochondria, JC-1 polymers) to green fluorescence (representing less activated mitochondria, JC-1 monomers). The imaging parameters remained consistent across all examined oocytes during image acquisition.

2.10. Measurement of intracellular ROS

Intracellular ROS level in the oocytes were measured using the ROS-sensitive fluorescent probe DCFH-DA (Beyotime Biotechnology Inc., China). In brief, oocytes were loaded with 5 μM DCFH-DA at 37 °C for 30 min, and then were washed three times using PBS to remove the surface fluorescence. The intensity of the fluorescence from each oocyte was measured by a fluorescence microscope (LSM 800, Zeiss, Germany) and quantified using ImageJ (National Institutes of Health, USA). The parameters used for image acquisition were similar for all examined oocytes.

2.11. Determination of Ca^{2+} level in oocytes

The intracellular Ca^{2+} levels within the oocytes were assessed utilizing the Ca^{2+}-sensitive fluorescent probe Fluo-4 AM (Beyotime Biotechnology Inc., China). Oocytes from each group were exposed to 5 μM Fluo-4 AM at 37 °C for 30 min and then underwent three washes with PBS to eliminate surface fluorescence. The fluorescence intensity within the intracellular oocytes was measured using a fluorescence microscope (LSM 800, Zeiss, Germany). Consistent imaging parameters were applied across all oocytes during the image acquisition process.

2.12. IVF and development of embryos

The procedures for in vitro fertilization and blastocyst culture are presented as follows. (1) Sperm capacitation: The male epididymis was surgically removed and placed in G-mops plus solution. Subsequently, the epididymal tail was dissected under a microscope to extract spermatozoa, which were then aspirated and capacitated for 1 h in HTF capacitation solution that had been equilibrated overnight. (2) Laser-assisted zona pellucida dissection of stage MII oocytes: Stage MII oocytes were immobilized in G-mops plus solution and precisely pierced using a micromanipulator equipped with a laser system to create perforations on the zona pellucida. Following this procedure, the oocytes were submerged again into G-mops plus solution. (3) In vitro fertilization: The perforated oocytes were transferred into HTF medium that had been equilibrated overnight, followed by addition of highly motile energized spermatozoa. Subsequently, the embryos were incubated for fertilization purposes within an incubator. After six hours, the resulting embryos were transferred to cleavage medium while recording rates of fertilization as well as development at stages including 2-cell, 4-cell, and blastocyst.

2.13. Statistical analysis

The data were presented as mean ± SD. GraphPad Software 8.0 was utilized for statistical analyses, employing either Student's *t*-test or one-way ANOVA. A significance level of $P < 0.05$ was considered statistically significant.

3. Results and discussion

3.1. Preparation, optimization, and characterization of MB@GBn

Firstly, an amphiphilic biodegradable nanocarrier GC-BR was synthesized as the presented reaction (Fig. 2A). This involved the conjugation of bilirubin to glycol chitosan through a carboxyl ammonia condensation reaction facilitated by EDC and NHS catalysis. The synthesized GC-BR was characterized using FTIR spectra (Fig. 2B) and ^1H NMR spectra (Fig. 2C). The reuslts indicated that the GC-BR conjugate was successfully synthesized.

Following that, we tested the self-assembly capacity of MT and BR. We tested four different BR/MT molar ratios, and the results showed that

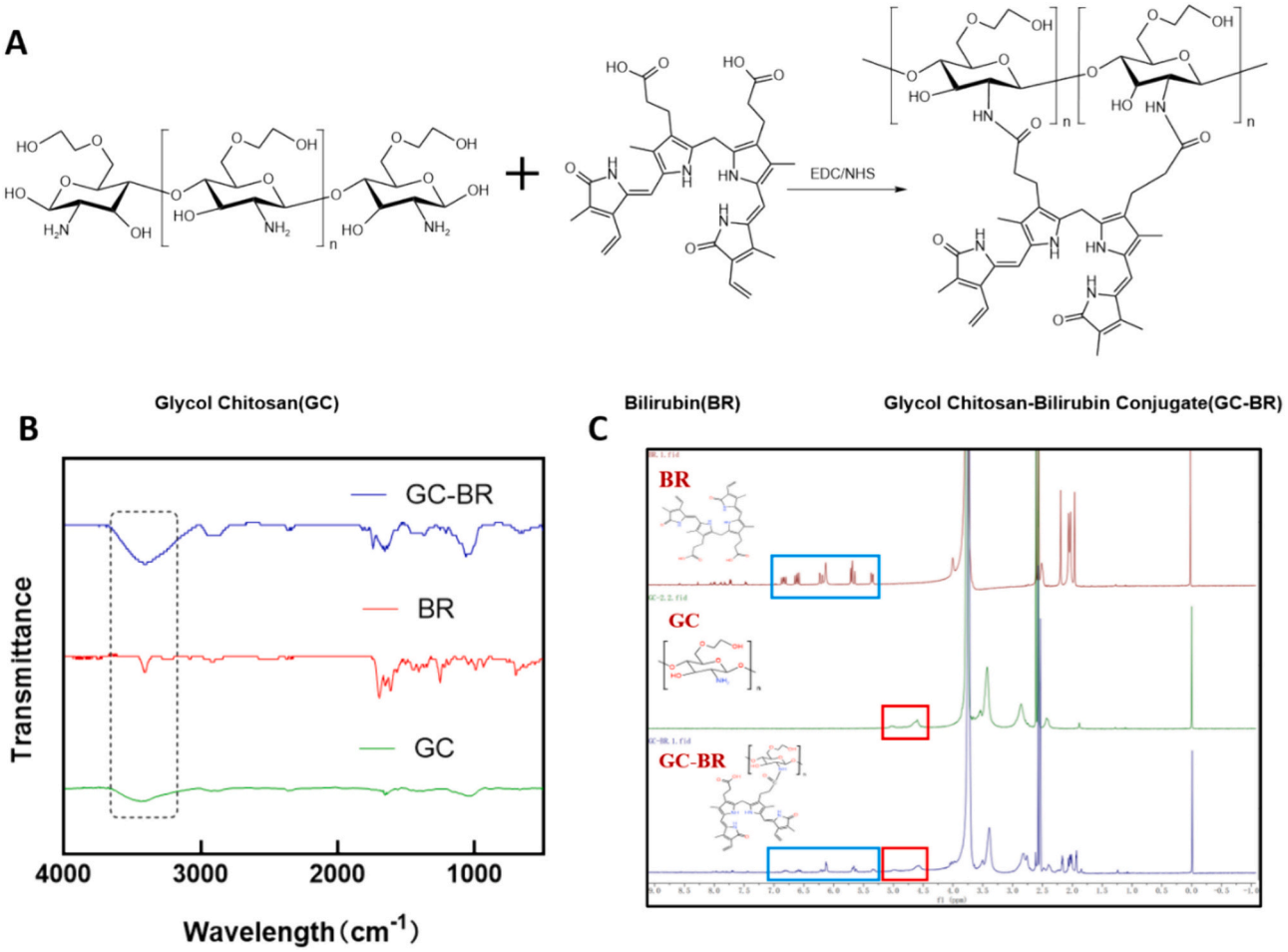

Fig. 2. Characterization of synthesized GC-BR. (A)Synthetic route of GC-BR. (B) Fourier transform infrared (FTIR) spectra and (C) ^{1}H nuclear magnetic resonance (NMR) spectra of GC-BR.

all these formulations could self-assembly into nanoparticles (Fig. 3A). Interestingly, the higher concentrations of BR led to larger particle sizes, reaching approximately 220 nm; conversely, when the concentration of melatonin surpassed that of bilirubin, the particle size was around 100 nm. All the PDI values were <0.25 and showed minimal differences between groups. For finer particles, we selected 1:5 of BR/MT ratio for the following experiments. DLS results showed the uniform and narrow distribution of MBn (1:5 of BR/MT ratio), and the zeta potential was −26.93 mV (Fig. 3C). We further investigated the stability of MBn when dispersed in distilled water. The results showed that MBn aggregated together in the third day, evidenced by the significantly increased particle size and PDI value (Fig. 3E).

To improve the stability of MBn, we then coated the nanoparticles with GC-BR conjugate. We tested different weight ratio (5%, 10%, 15%, 20%, 25% *w*/w) of GC-BR/MBn (Fig. 3B). When 5% GC-BR was added in the formulation, the nanoparticles would aggregate, and the particle size was increased up to 900 nm. This outcome might be attributed to the insufficient presence of GC-BR, unable to effectively adhere to the inner core's surface, leading to system destabilization. With the ratio increased, the particle size decreased; when the ratio was over 20%, the particle size would not decreased any more. In addition, with the addition of GC-BR, the zeta potential of nanoparticles were increased to the positive. Usually, chitosan always showed positive potential when formulated into nanoparticles due to the residual amino groups (Chen et al., 2023). Considering the experimental outcomes, our aim to achieve optimal drug delivery and higher drug utilization while practicing conservation and environmental protection, led us to select the 20% MB@GBn formulation as the final nanoparticle configuration for further biological evaluation. DLS reuslts showed that MB@GBn also showed unifom distribution (PDI = 0.1807), and the zeta potential was increased up to 11.35 mV (Fig. 3D). After coating, the nanoparticle size was increased from 85 nm to 128 nm, and the zeta potential was increased from −26.93 mV to 11.5 mV, indicating the successful coating. This change might be attributed to the electrostatic attraction between the negatively charged MB and the positively charged GC-BR, allowing GB to adhere to the MB surface and augment the particle size. Figs. 3F display the seven-day stability of MB@GBn, including particle size and PDI. It's evident that the long-term stability of MB@GBn surpassed that of MB. These results also signified that the presence of GC-BR as a carrier significantly improved the stability of MBn.

TEM analysis showcased the spherical shape of MB@GBn (Fig. 4A), albeit slightly smaller in size compared to the measurements obtained via the DLS method. This difference could be attributed to the drying process under TEM versus the aqueous dispersion utilized for DLS analysis. Moreover, MB@GBn showed significant structural alterations under hydrogen peroxide exposure, indicating the ROS-responsiveness (Fig. 4B). In addition, DLS results also suggested an unstable particle size in the presence of hydrogen peroxide, showcasing a dual peak and signaling structural dissociation with a considerable increase in particle size (Fig. 4C). The release behavior of MB@GBn was investigated in the presence or absence of H_2O_2 (Fig. 4D). Due to that BR was easily oxidized and therefore hard for quantification, MT was served as an indicator for the release profiles of MB@GBn. The graph illustrated that free MT was rapidly released, with over 80% released within approximately 24 h. Notably, the addition of H_2O_2 significantly accelerated the release rate of MB@GBn, reaching around 80% release after 48 h.

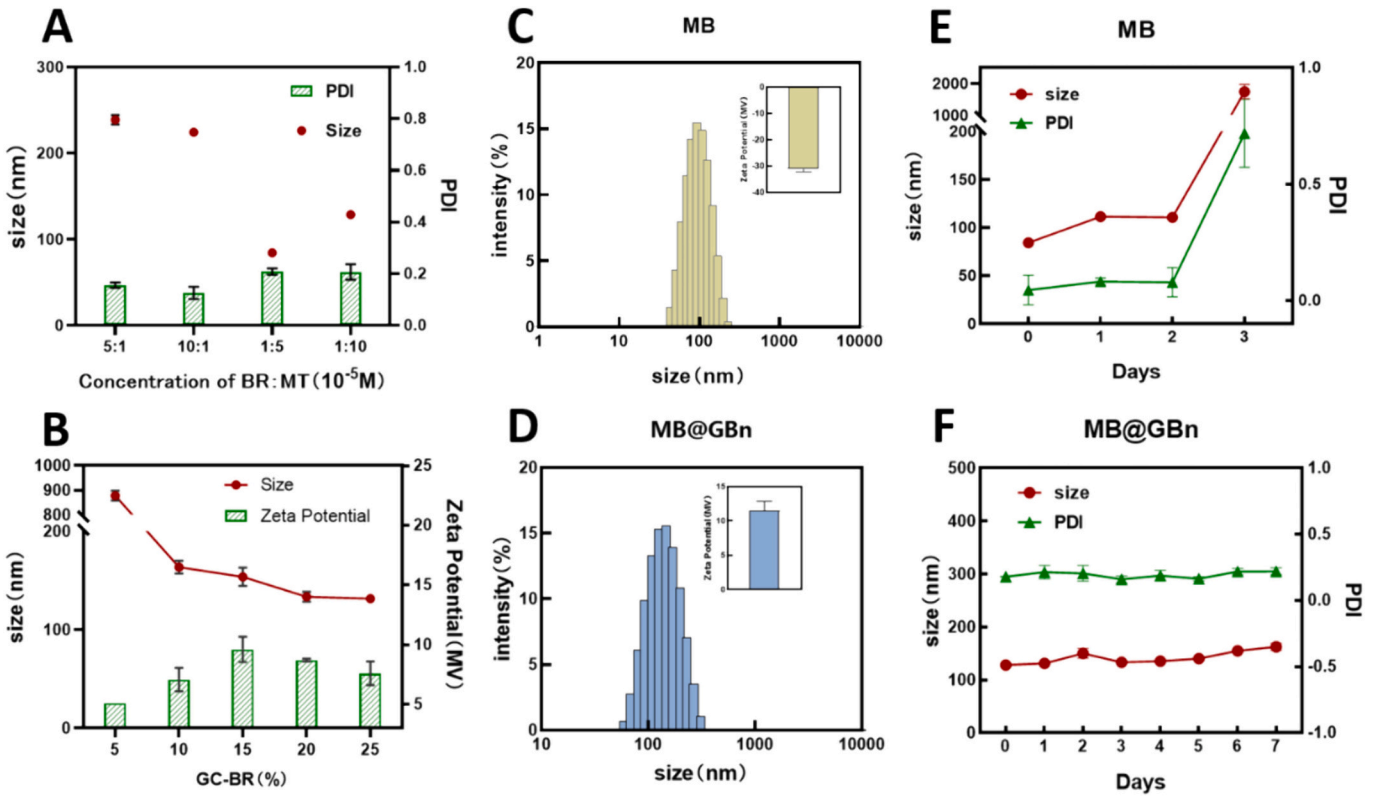

Fig. 3. Optimization and characterization of MB@GBn. (A) Particle size and PDI of MB at different molar ratio of BR/MT. (B) Particle size and zeta potential of MB@GBn at different ratio of GC-BR/BMn. (C) Particle size and zeta potential of optimized MBn. (D) Particle size and zeta potential of optimized MB@GBn. (E) Stability of MBn. (F) Stability of MB@GBn. Data are shown in Mean ± SD ($n = 3$).

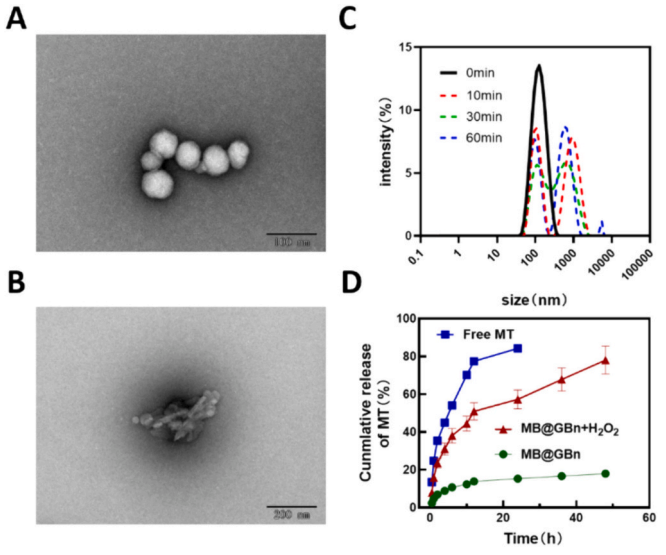

Fig. 4. ROS-responsive characteristics of MB@GBn. TEM image of MB@GBn (A) in the absence or (B) in the presence of 0.3% H_2O_2. (C) The particle size distribution variation of MB@GBn in the presence of 0.3% H_2O_2 along with time. (D) The cumulative release of free MT and MT from MB@GB in the presence or absence of 0.3% H_2O_2 in pH 7.4 PBS containing 0.5% Tween 80 at 37 °C ($n = 3$).

Conversely, in the absence of H_2O_2, MB@GBn exhibited a slower release pattern. These results demonstrated the ROS-responsive behavior of MB@GBn, which could be attributed to the bilirubin core. Under ROS-rich conditions, the hydrophobic bilirubin likely undergoes oxidation, transforming into hydrophilic bilirubin, thereby disassembling the nanoparticle and initiating drug release (Yao et al., 2020e). These results suggested MB@GBn disassembles under ROS-rich conditions to release loaded drugs. Additionally, the MT encapsulation efficiency (EE) and drug load (DL) in MB@GBn were determined as 70.1% and 38.7%, respectively.

3.2. *The biocompatibility of MB@GBn and its effect on oocyte maturation*

The in vitro toxicity assessment of MB@GBn on HUVEC cells was conducted using the MTT method. Notably, when BR concentrations ranged from 1 to 10 μM, the cell viability was observed within the range of 72% to 80% (Fig. 5A) The slightly decrease in cell viability might be due to the low solubility of BR and the sediment affecting cell growth. Meanwhile, for MT concentrations spanning from 5 to 50 μM, the viability reached approximately 90% or higher (Fig. 5B). For MB@GBn, neglectable decrease was observed, similar as MT, indicating the favorable biocompatibility and low toxicity (Fig. 5C). these results suggested that nanoparticle strategy addressed the low solubility of BR induced cell viability decrease and improved the draggability of BR.

After verifying the safety of MB@GBn, we proceeded to assess its efficacy (Fig. 5D). GV stage oocytes were obtained from 4-week-old female ICR mice post-ovulation induction and were categorized into different groups: the control group, which included IOs (inferior oocytes) and COCs (cumulus cells retained); the experimental group consisting of various concentrations of MB@GBn (0.5, 1, 2.5 × 10^{-5} M, expressed as MT concentration in MB@GBn). The granulosa cell, being the predominant cell population within the follicle, plays a pivotal role in supporting the oocyte, its abundance being intricately linked to oocyte quality. These cells produce various substances that act as nutrients, crucial for nurturing the growth and maturation of the oocyte (Canipari, 2000; Richani et al., 2021). Therefore, IOs and COCs were selected as controls. During in vitro maturation (IVM), oocytes from the

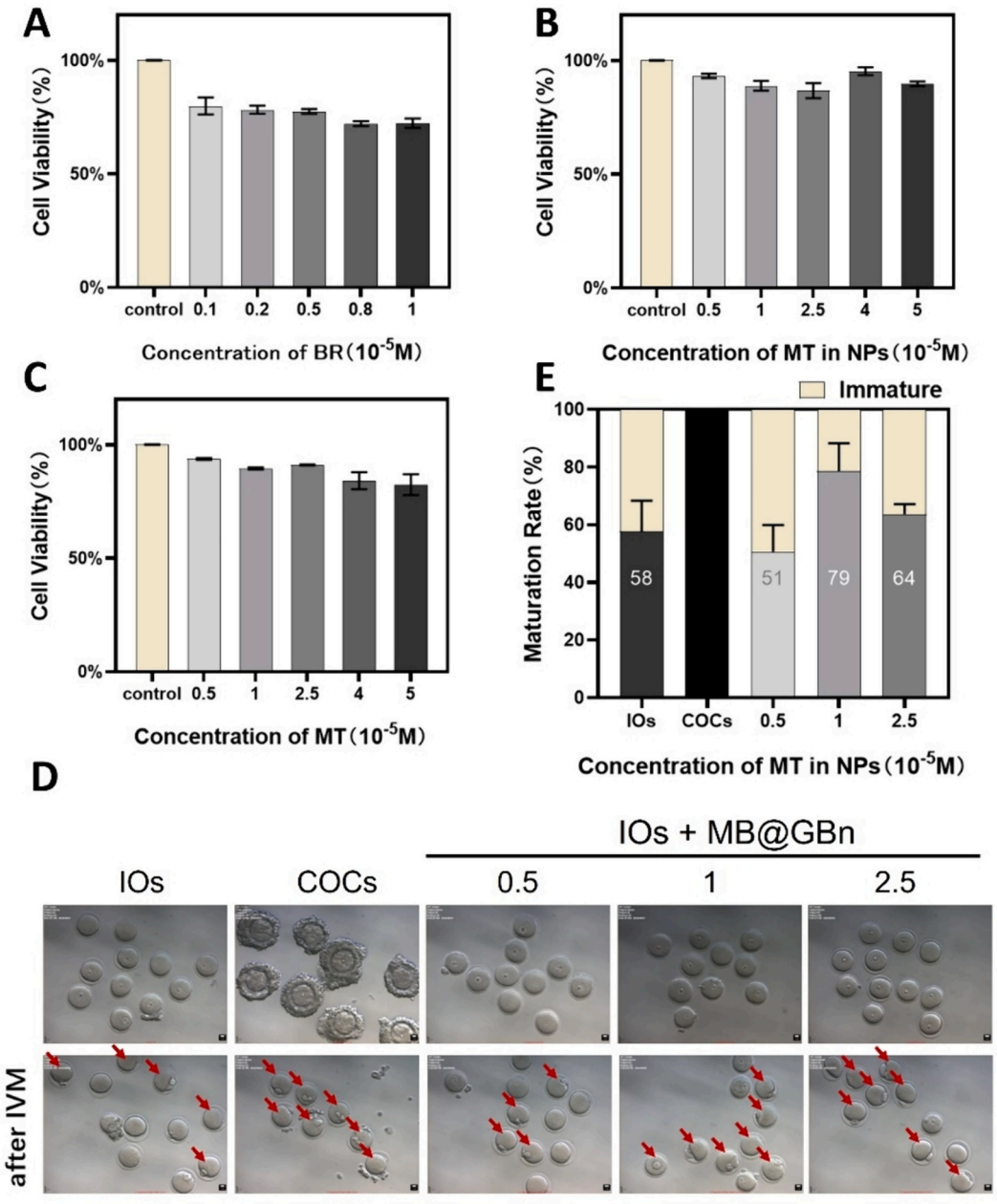

Fig. 5. Cell viability and enhancing IVM efficacy of MB@GBn. (A) Cell viability of HUVEC cells after treatment with different concentration of BR, or (B) MT, or (C) MB@GBn. (D)Diagram of oocytes before and after MB@GBn's treatment, the red arrows indicate mature oocytes (scale bar = 10 μm). (E) Maturation rate of oocytes in different groups. (For interpretation of the references to colour in this figure legend, the reader is referred to the web version of this article.)

experimental group were treated with different MB@GBn concentrations, progressing through GVBD, MI, and finally reaching the M II stage, indicative of mature oocytes suitable for IVF or ICSI. Analysis of the oocyte images post-IVM revealed that the maturation rate (Fig. 5E) in the IOs group was only 58%, whereas COCs exhibited a 100% maturation rate, mirroring in vivo conditions where cumulus cells were preserved, ensuring healthier oocyte development. In vitro fertilization treatments involving oocytes removed from their in vivo environment and support structures showed reduced maturation rates. However, the addition of MB@GBn to IOs resulted in a 79% maturation rate at a 10 μM MT concentration within MB@GBn, surpassing the IOs group. This outcome underscored the substantial role of MB@GBn treatment. Consequently, this concentration was selected for subsequent therapeutic applications in our study.

3.3. The uptake profiles of MB@GBn in HUVEC and mouse oocytes

Based on the impressive results, we further investigated the uptake behaviors of MB@GBn after incubating with HUVEC or mouse oocytes, and coumarin 6 (C6) was selected as a probe. As shown in Fig. 6A&B, we monitored the uptake of MB@GBn on HUVEC cells within 4 h. With the incubation time increasing, the intracellular fluorescence intensity in HUVEC increased, indicating the time-dependent uptake profiles within 4 h. We further investigated the uptake profiles of MB@GBn in mouse oocytes (Fig. 6C&D). The results also showed a time-dependent trend. However, the uptake amount of MG@GBn in oocytes was much lower than that in HUVEC cells. This might be due to the zona pellucida surrounding oocytes restricting the uptake of MB@GBn to a certain exert. Even so, with the uptake rate, MB@GBn was sufficient to promote oocyte maturation for IOs.

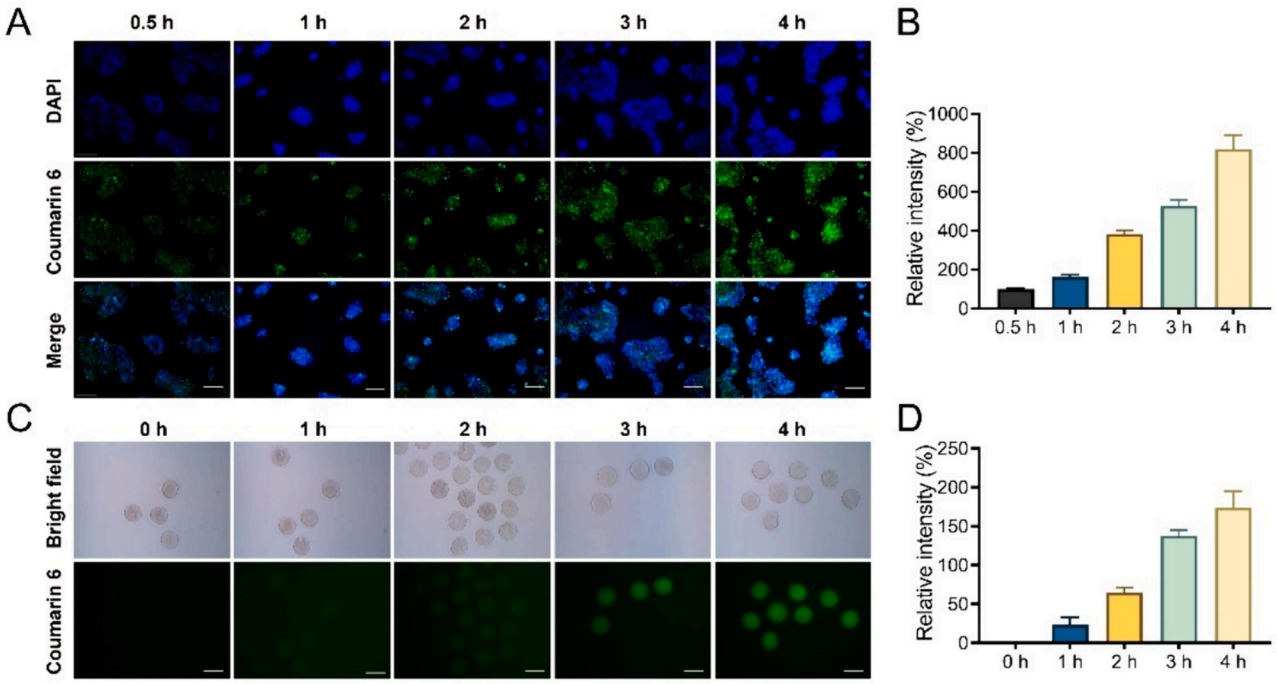

Fig. 6. The uptake profiles of MB@GBn in HUVEC cells and mouse oocytes. Coumarin 6 was selected as a fluorescence probe for monitoring the uptake of nanoparticles. (A) The representative images indicating the uptake of C6-loaded MB@GBn in HUVEC cells (scale bar = 100 μm) and (B) the quantitative analysis. (C) The representative images indicating the uptake of C6-loaded MB@GBn in mouse oocytes (scale bar = 100 μm) and (D) the quantitative analysis.The average fluorescence intensity for MB@GBn in HUVEC at 0.5 h was used as 100%, and the relative results were calculated in the other groups. Data presented as mean ± SD (n = 3).

3.4. MB@GBn improving the quality of mouse IVM-MII oocytes

To assess the impact of MB@GBn supplementation on oocyte maturation in vitro, germinal vesicle (GV) oocytes were cultured using an in vitro maturation medium, and subsequently, the collected metaphase II (MII) oocytes were studied. To further investigate the influence of MB@GBn supplementation on the quality of mouse IVM-MII oocytes, we evaluated intracellular levels of ROS, MMP, and Ca^{2+}, crucial factors associated with oocyte quality and developmental capability.

ROS, essential byproducts of various biochemical reactions within cell organelles, play a pivotal role in nuclear maturation, dependent on oxidative phosphorylation and oxygen supply in oocytes. However, excessive ROS production impedes oocyte growth, leading to oxidative stress and disrupting mitochondrial function. Maintaining a balance between ROS generation and antioxidative capacity is crucial for oocyte development and quality. The intracellular ROS level greatly influences spindle formation, chromosome sequencing, and oocyte maturation. IOs showed significantly increased ROS level compared to COCs (Fig. 7). Notably, following exposure to MB@GBn, there was a significant decrease in the relative fluorescence intensity of ROS. Each component could suppress the ROS production, and the ROS level in oocytes of MB@GBn group were even lower than that in COCs group. These results

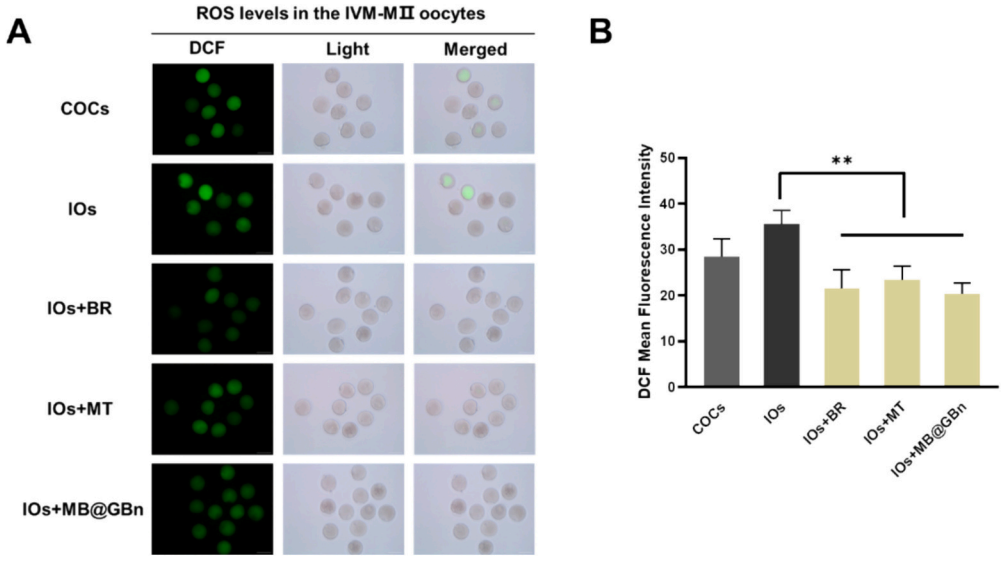

Fig. 7. The effect of MB@GBn on the intracellular ROS of oocytes. (A) Representative images of ROS in mouse oocytes (scale bar = 100 μm). (B) Quantitative analysis of fluorescence intensity in mouse oocytes (n = 3). Data are shown in Mean ± SD. **, $P < 0.01$, indicating statistical difference between groups as indicated.

demonstrated the potent antioxidant property of MB@GBn.

During maturation onset (germinal vesicle breakdown, GVBD), calcium signals play critical roles (Campos et al., 2023; Whitaker, 2006). Calcium, as a critical second messenger in cells, significantly influences oocyte maturation and fertilization. The intracellular Ca^{2+} level serves as an indicator of mitochondrial function, as mitochondria regulate calcium storage and maintain calcium homeostasis in oocytes. In comparison with the IOs group, treatment with MB@GBn significantly reduced the intracellular calcium level ($P < 0.01$) (Fig. 8). Here, although each component showed inhibitory effect on the intracellular Ca^{2+} to some extent, MB@GBn showed remarkably enhanced effect. BR showed potent antioxidative property but was less effective in suppressing intracellular calcium level in oocytes; while MT was more effective in reducing Ca^{2+} level compared to scavenging ROS; the combination of BR and MT in the nanoparticle form exerted synergistic effect to retain the oocyte quality.

Sufficient ATP is crucial for continuous transcription and translation during oocyte maturation, making the presence of an appropriate number of functional mitochondria vital (Kirillova et al., 2021). MMP stands as a pivotal indicator reflecting mitochondrial function, closely linked to oocyte development. Positive correlations have been established between oocyte development and mitochondrial functionality. To assess mitochondrial function, we measured the MMP of oocytes. The JC-1 monomer emits green fluorescence in the FITC channel (indicative of low polarized mitochondria), while the JC-1 polymer emits red fluorescence (indicative of highly polarized mitochondria). The relative levels of red to green fluorescence were used to assess mitochondrial polarization. As shown in Fig. 9, a significant difference was observed between the IOs group and the MB@GBn group. Notably, treatment with MB@GBn led to an increase in the MMP level in oocytes compared to the IOs group. Interestingly, BR exerted potent effect on scavenging ROS and modulating MMP but was less effective in regulating intracellular Ca^{2+} level, while MT showed considerable effect on all these aspects. MB@GBn showed robust effect to modulate IOs to healthy state.

These results display notable distinctions in the levels of intracellular ROS, MMP, and Ca^{2+} between the cumulus-oocyte complexes (COCs) culture group and the IOs culture group. Quantitative analysis revealed a marked increase in the relative fluorescence intensity of ROS and Ca^{2+} in the IOs group, while the MMP level notably decreased in the same group. These observations suggest that in vitro culture of degranulated cells has an adverse effect on oocyte quality. However, fluorescence staining revealed the levels of ROS, Ca^{2+}, and MMP in the IVM-MII oocytes, highlighting the impact of MB@GBn treatment on oocyte quality and maturation compared to the IOs group. We observed a significant decrease in ROS and Ca^{2+} levels in oocytes treated with MB@GBn, alongside a noteworthy increase in MMP. These outcomes strongly suggest an enhancement in oocyte quality and maturation. Our findings indicated lower levels of intracellular ROS and Ca^{2+} in the MB@GBn-treated groups compared to the IOs groups, while MMP levels in these treated oocytes were higher than those in the IOs groups and similar to those in the COCs groups. Based on these findings, the MB@GBn treatment effectively preserved oocyte quality during IVM culture.

3.5. MB@GBn did not affect IVF and development of embryos

Clinically, in vitro maturation culture is employed to obtain more mature oocytes for IVF. Therefore, we investigated the impact of MB@GBn addition on subsequent IVF and embryo development in mouse oocytes. The fertilization and developmental outcomes were compared among different groups after IVF. Optical microscope images revealed that the addition of MB@GBn did not significantly affect the morphological characteristics of embryos; their cells appeared spherical and glossy without evident degeneration (Fig. 10A). The COCs group ($n = 128$) exhibited a fertilization rate of (51.96 ± 5.23)%, while the MB@GBn group ($n = 108$) showed a rate of (52.71 ± 6.34)% (Fig. 10B). Moreover, the cleavage rates were found to be (84.75 ± 5.59)% for the COCs group and (83.33 ± 15.27)% for the MB@GBn group, respectively (Fig. 10C). Similarly, blastocyst rates were observed to be (40 ± 10)% for COCs group and (43.45 ± 6.27)% for MB@GBn group following IVF procedures (Fig. 10D). Compared to the COCs group, there were no statistically significant differences observed in the rates of fertilization, cleavage, and blastocyst formation following IVF. In conclusion, the addition of MB@GBn can enhance oocyte maturation without impacting the fertilization competence and developmental potential of mature oocytes.

4. Discussion

Even though many compounds from herb medicine have shown potent capacity to scavenge overproduced ROS (Kaur et al., 2022; Qin et al., 2022; Tai et al., 2022; Chen et al., 2022b), the endogenous

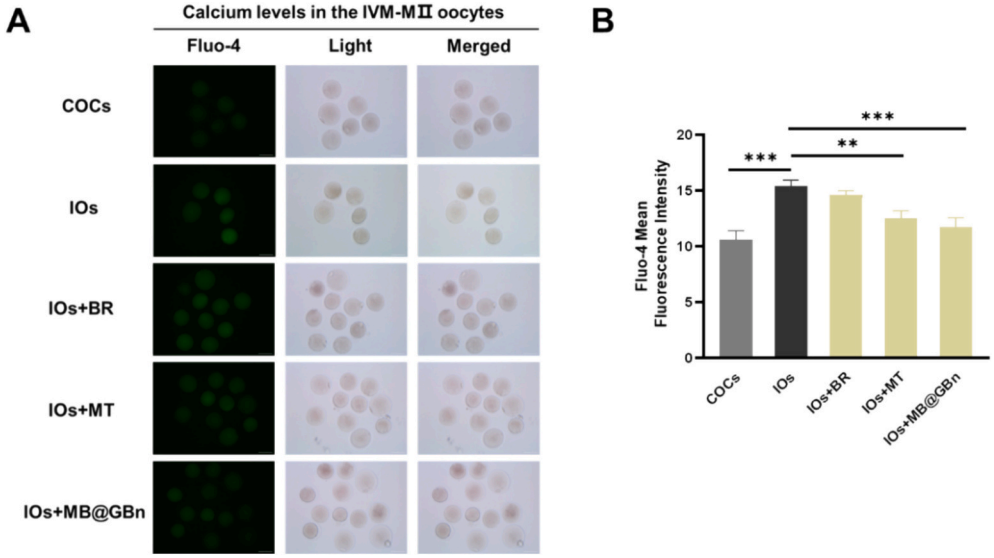

Fig. 8. Evaluation of MB@GBn effect on oocytes. (A) Representative images of Fluo-4 AM fluorescence (green) in mouse oocytes (scale bar = 100 μm). (B) Quantification of the relative levels of Ca^{2+} in mouse oocytes ($n = 3$). Data are shown in Mean ± SD. **, $P < 0.01$, ***, $P < 0.001$, indicating statistical difference between groups as indicated. (For interpretation of the references to colour in this figure legend, the reader is referred to the web version of this article.)

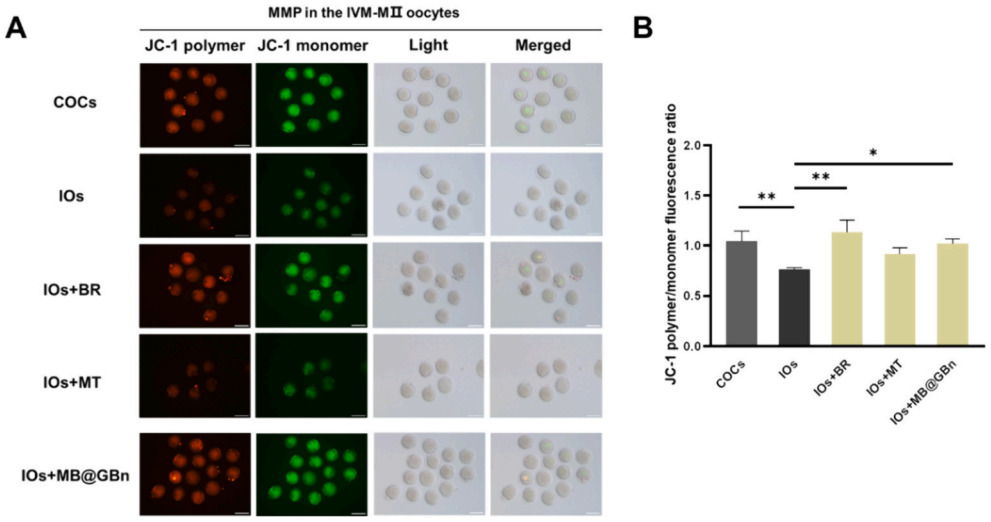

Fig. 9. Evaluation of MB@GBn effect on oocytes. (A) Representative images of MMP in mouse oocytes stained with JC-1 (scale bar = 100 μm). (B) MMP levels (red/green fluorescence intensity) were detected in mouse oocytes ($n = 3$). Data are shown in Mean ± SD. *, $P < 0.05$, **, $P < 0.01$, indicating statistical difference between groups as indicated. (For interpretation of the references to colour in this figure legend, the reader is referred to the web version of this article.)

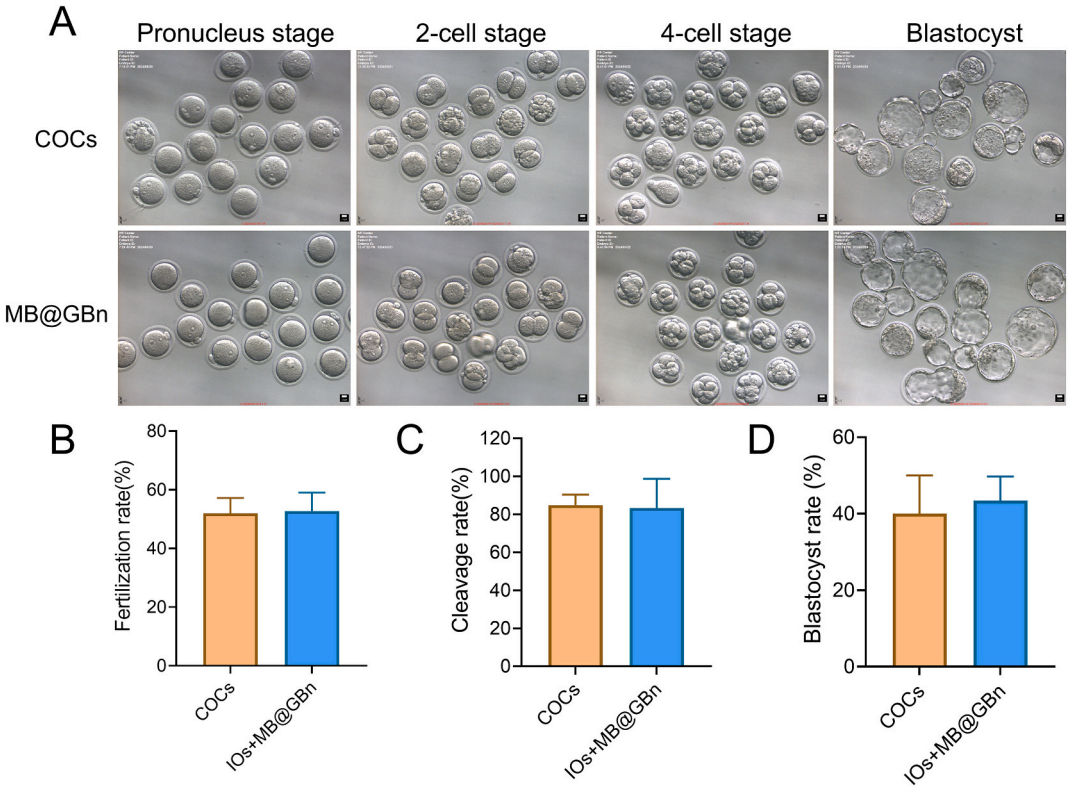

Fig. 10. Evaluation of MB@GBn on fertilization competence and oocyte development. (A) The morphology of oocyte after IVF and development (scale bar = 10 μm). (B) The fertilization rate, (C) cleavage rate, and (D) blastocyst rate of oocytes in the absence and presence of MB@GBn.

property of melatonin and bilirubin makes them more potential for IVF application, especially the ideal safety. The existing body of research demonstrates the favorable impacts of melatonin on reproductive processes. As a safe and natural small molecule medicine, melatonin possesses essential antioxidant and anti-inflammatory properties, contributing to the enhancement of oocyte quality and maturation (Chuffa et al., 2021; He et al., 2016). Nevertheless, these studies have primarily focused on the application of melatonin in its singular form. Despite the promising therapeutic potential of melatonin, its inherent limitations should not be disregarded, such as its specific solvent requirements, poor water solubility, and short half-life, imposing constraints on its utilization. Similarly, bilirubin was also a star compound in relieving ROS, inhibiting inflammation, and modulating immune reaction. But its low solubility severely restricts its further application.

Our study aimed to develop a nanocarrier system to address these shortcomings and enable a more efficient harnessing of the therapeutic effects of these two compounds. During the experiment, we found the carrier-free nanoparticles by assembling melatonin and bilirubin were not stable enough for further biological application. We further synthesized bilirubin-grafted chitosan (GC-BR) to coat and stabilize

melatonin/bilirubin nanoparticles. The synthesized GC-BR could coat the nanoparticles by bilirubin-match property, evidenced by the reversed zeta potential. In addition, the stability of new formed nanoparticles, MB@GBn, was significantly enhanced. The nanoparticles were designed to dissolve in water rather than organic solvents, ensuring high solubility and favorable biosafety as well as addressing the limitations of themselves. Crucially, the nanoparticle displays ROS-responsive features. In environments with high ROS levels, the outer shell disintegrates gradually, allowing the controlled release of melatonin and bilirubin. This feature eliminates the need for multiple dosing, enhancing the clinical feasibility and practicality of this approach.

Extensive research has underscored the profound impact of environmental changes during oocyte development on the subsequent stages of zygote development (Dvoran et al., 2022; He et al., 2021). Oocyte maturation encompasses a multifaceted process entailing cell cycle regulation, spindle assembly mediated by microtubules, chromosome segregation, organelle redistribution, spindle migration via microfilament backbone, and cytoplasmic division (Coticchio et al., 2015). Alterations in environmental factors could influence morphological changes, gene recombination, epigenetic modifications, and germ cell metabolism, consequently impacting the zygote, embryo development, and potentially the long-term health of the offspring (Dvoran et al., 2022; Sales et al., 2017; Telfer et al., 2023). Notably, our evaluation of MB@GBn's efficacy was confined to not only the oocyte level, but also extending to appraise zygote quality and subsequent developmental stages. The addition of MB@GBn demonstrates effectiveness in mitigating high ROS risks during IVM, as well as its negligible impact on oocytes and subsequent embryo development. Our results confirmed the potential benefits concerning oocyte maturation and drug's safety in oocyte fertilization and embryo development. Nonetheless, it's important to acknowledge the limitations of this study, primarily that our evaluation of MB@GBn's efficacy was confined to the oocyte level, fertilization, and developmental stages, without extending to appraise pregnancy rate and baby growth/development. Consequently, future studies will prioritize assessing the effects of MB@GBn on pregnancy rate and baby growth/development to further confirm the benefits. This comprehensive evaluation aims to establish a robust safety and efficacy assessment framework, offering a new approach to optimize IVM and enhance oocyte quality.

5. Conclusion

In this study, we developed nanoparticles by self-assembling endogenous bilirubin and melatonin hormone coated with bilirubin-conjugated glycol chitosan (MB@GBn) to alleviate oxidative stress and enhance oocyte maturation and quality during IVM. These nanoparticles could adhere to the oocyte surface by electrostatic interaction for immediate protection. MB@GBn treatment showed potent effect in suppressing ROS production, inhibiting calcium ions, and improving mitochondrial membrane potential, collectively contributing to an enhancement in the quality of IOs. Consequently, the application of MB@GBn demonstrates promise as an effective therapeutic strategy for IVM.

CRediT authorship contribution statement

Haitao Xi: Methodology, Investigation. **Lihui Huang:** Writing – original draft, Investigation. **Lin Qiu:** Methodology. **Shize Li:** Resources. **Yuqi Yan:** Software. **Yang Ding:** Validation. **Yuhao Zhu:** Visualization. **Fugen Wu:** Resources. **Xianbao Shi:** Methodology, Resources. **Junzhao Zhao:** Formal analysis. **Ruijie Chen:** Supervision. **Qing Yao:** Writing – review & editing, Conceptualization. **Longfa Kou:** Writing – review & editing, Supervision, Project administration, Funding acquisition, Conceptualization.

Declaration of competing interest

The authors declare that they have no known competing financial interests or personal relationships that could have appeared to influence the work reported in this paper.

Data availability

Data will be made available on request.

Acknowledgments

This research was supported by Zhejiang Medical and Health Science and Technology Program (2022KY881, 2023KY884), Science & Technology Innovation Project of Wenzhou (ZY2019007, Y20220908), and Excellent Young Scientist Training Program fund from Wenzhou Medical University. We also acknowledge the Scientific Research Center of Wenzhou Medical University for consultation and instrument availability that supported this work.

References

Abecia, J.A., Forcada, F., Zúñiga, O., 2002. The effect of melatonin on the secretion of progesterone in sheep and on the development of ovine embryos in vitro. Vet. Res. Commun. 26 (2), 151–158.
Agarwal, A., Durairajanayagam, D., du Plessis, S.S., 2014. Utility of antioxidants during assisted reproductive techniques: an evidence based review. Reprod. Biol. Endocrinol. 12, 112.
Brown, H.M., Dunning, K.R., Sutton-McDowall, M., Gilchrist, R.B., Thompson, J.G., Russell, D.L., 2017. Failure to launch: aberrant cumulus gene expression during oocyte in vitro maturation. Reproduction 153 (3), R109–r120.
Campos, G., Sciorio, R., Esteves, S.C., 2023. Total fertilization failure after ICSI: insights into pathophysiology, diagnosis, and management through artificial oocyte activation. Hum. Reprod. Update 29 (4), 369–394.
Canipari, R., 2000. Oocyte—granulosa cell interactions. Hum. Reprod. Update 6 (3), 279–289.
Carson, S.A., Kallen, A.N., 2021. Diagnosis and Management of Infertility: a Review. Jama 326 (1), 65–76.
Chen, R., Zhai, Y.-Y., Sun, L., Wang, Z., Xia, X., Yao, Q., Kou, L., 2022a. Alantolactone-loaded chitosan/hyaluronic acid nanoparticles suppress psoriasis by deactivating STAT3 pathway and restricting immune cell recruitment. Asian Journal of Pharmaceutical Sciences 17 (2), 268–283.
Chen, R., Sun, G., Xu, L., Zhang, X., Zeng, W., Sun, X., 2022b. Didymin attenuates doxorubicin-induced cardiotoxicity by inhibiting oxidative stress. Chinese Herbal Medicines 14 (1), 70–78.
Chen, R., Lin, X., Wang, Q., An, X., Zhao, X., Lin, Y., Sun, T., Yan, C., Cai, A., Cao, W., Zhang, Y., Yao, Q., Kou, L., 2023. Dual-targeting celecoxib nanoparticles protect intestinal epithelium and regulate macrophage polarization for ulcerative colitis treatment. Chem. Eng. J. 452, 139445.
Chen, R., Jiang, Z., Cheng, Y., Ye, J., Li, S., Xu, Y., Ye, Z., Shi, Y., Ding, J., Zhao, Y., Zheng, H., Wu, F., Lin, G., Xie, C., Yao, Q., Kou, L., 2024. Multifunctional iron-apigenin nanocomplex conducting photothermal therapy and triggering augmented immune response for triple negative breast cancer. Int. J. Pharm. 655, 124016.
Chian, R.C., Uzelac, P.S., Nargund, G., 2013. In vitro maturation of human immature oocytes for fertility preservation. Fertil. Steril. 99 (5), 1173–1181.
Choi, J., Park, S.M., Lee, E., Kim, J.H., Jeong, Y.I., Lee, J.Y., Park, S.W., Kim, H.S., Hossein, M.S., Jeong, Y.W., Kim, S., Hyun, S.H., Hwang, W.S., 2008. Anti-apoptotic effect of melatonin on preimplantation development of porcine parthenogenetic embryos. Mol. Reprod. Dev. 75 (7), 1127–1135.
Chuffa, L.G.A., Seiva, F.R.F., Novais, A.A., Simão, V.A., Martín Giménez, V.M., Manucha, W., Zuccari, D., Reiter, R.J., 2021. Melatonin-Loaded Nanocarriers: New Horizons for Therapeutic applications. Molecules 26 (12).
Cipolla-Neto, J., Amaral, F.G.D., 2018. Melatonin as a Hormone: New Physiological and Clinical Insights. Endocr. Rev. 39 (6), 990–1028.
Coticchio, G., Dal Canto, M., Mignini Renzini, M., Guglielmo, M.C., Brambillasca, F., Turchi, D., Novara, P.V., Fadini, R., 2015. Oocyte maturation: gamete-somatic cells interactions, meiotic resumption, cytoskeletal dynamics and cytoplasmic reorganization. Hum. Reprod. Update 21 (4), 427–454.
De Vos, M., Smitz, J., Thompson, J.G., Gilchrist, R.B., 2016. The definition of IVM is clear-variations need defining. Hum. Reprod. 31 (11), 2411–2415.
De Vos, M., Grynberg, M., Ho, T.M., Yuan, Y., Albertini, D.F., Gilchrist, R.B., 2021. Perspectives on the development and future of oocyte IVM in clinical practice. J. Assist. Reprod. Genet. 38 (6), 1265–1280.
Duffy, D.M., Ko, C., Jo, M., Brannstrom, M., Curry, T.E., 2019. Ovulation: parallels with inflammatory processes. Endocr. Rev. 40 (2), 369–416.
Dvoran, M., Nemcova, L., Kalous, J., 2022. An Interplay between Epigenetics and translation in Oocyte Maturation and embryo Development: Assisted Reproduction Perspective. Biomedicines 10 (7).

Fischer, B., Bavister, B.D., 1993. Oxygen tension in the oviduct and uterus of rhesus monkeys, hamsters and rabbits. J. Reprod. Fertil. 99 (2), 673–679.
He, C., Wang, J., Zhang, Z., Yang, M., Li, Y., Tian, X., Ma, T., Tao, J., Zhu, K., Song, Y., Ji, P., Liu, G., 2016. Mitochondria Synthesize Melatonin to Ameliorate its Function and Improve mice Oocyte's Quality under in Vitro Conditions. Int. J. Mol. Sci. 17 (6).
He, M., Zhang, T., Yang, Y., Wang, C., 2021. Mechanisms of Oocyte Maturation and Related Epigenetic Regulation. Frontiers in Cell and Developmental Biology 9.
Huang, Z.W., Shi, Y., Zhai, Y.Y., Du, C.C., Zhai, J., Yu, R.J., Kou, L., Xiao, J., Zhao, Y.Z., Yao, Q., 2021. Hyaluronic acid coated bilirubin nanoparticles attenuate ischemia reperfusion-induced acute kidney injury. J. Control. Release 334, 275–289.
Huang, H., Zheng, S., Wu, J., Liang, X., Li, S., Mao, P., He, Z., Chen, Y., Sun, L., Zhao, X., Cai, A., Wang, L., Sheng, H., Yao, Q., Chen, R., Zhao, Y.Z., Kou, L., 2024. Opsonization Inveigles Macrophages Engulfing Carrier-Free Bilirubin/JPH203 Nanoparticles to Suppress Inflammation for Osteoarthritis Therapy, Advanced Science. Baden-Wurttemberg, Germany, Weinheim, p. e2400713.
Ishizuka, B., Kuribayashi, Y., Murai, K., Amemiya, A., Itoh, M.T., 2000. The effect of melatonin on in vitro fertilization and embryo development in mice. J. Pineal Res. 28 (1), 48–51.
Jiang, X., Yao, Q., Xia, X., Tang, Y., Sun, M., Li, Y., Zheng, H., Cai, A., Zhang, H., Ganapathy, V., Chen, R., Kou, L., 2022. Self-assembled nanoparticles with bilirubin/JPH203 alleviate imiquimod-induced psoriasis by reducing oxidative stress and suppressing Th17 expansion. Chem. Eng. J. 431, 133956.
Jiang, X., Huang, S., Cai, W., Wang, P., Jiang, Z., Wang, M., Zhang, L., Mao, P., Chen, L., Wang, R., Sun, T., Jiang, Y., Yao, Q., Chen, R., Kou, L., 2023. Glutamine-based metabolism normalization and oxidative stress alleviation by self-assembled bilirubin/V9302 nanoparticles for psoriasis treatment. Adv. Healthc. Mater. 12 (13), 2203397.
Kaur, K., Sharma, R., Singh, A., Attri, S., Arora, S., Kaur, S., Bedi, N., 2022. Pharmacological and analytical aspects of alkannin/shikonin and their derivatives: An update from 2008 to 2022. Chinese Herbal Medicines 14 (4), 511–527.
Kirillova, A., Smitz, J.E.J., Sukhikh, G.T., Mazunin, I., 2021. The Role of Mitochondria in Oocyte Maturation. Cells 10 (9).
Kou, L., Huang, H., Tang, Y., Sun, M., Li, Y., Wu, J., Zheng, S., Zhao, X., Chen, D., Luo, Z., Zhang, X., Yao, Q., Chen, R., 2022a. Opsonized nanoparticles target and regulate macrophage polarization for osteoarthritis therapy: a trapping strategy. J. Control. Release 347, 237–255.
Kou, L., Jiang, X., Tang, Y., Xia, X., Li, Y., Cai, A., Zheng, H., Zhang, H., Ganapathy, V., Yao, Q., Chen, R., 2022b. Resetting amino acid metabolism of cancer cells by ATB(0,+)-targeted nanoparticles for enhanced anticancer therapy. Bioact Mater 9, 15–28.
Li, S., Zhang, W., Zhu, Y., Yao, Q., Chen, R., Kou, L., Shi, X., 2024. Nanomedicine revolutionizes epilepsy treatment: overcoming therapeutic hurdles with nanoscale solutions. Expert Opin. Drug Deliv. 21, 735–750.
Liang, S., Guo, J., Choi, J.W., Kim, N.H., Cui, X.S., 2017. Effect and possible mechanisms of melatonin treatment on the quality and developmental potential of aged bovine oocytes. Reprod. Fertil. Dev. 29 (9), 1821–1831.
Ng, K.Y.B., Mingels, R., Morgan, H., Macklon, N., Cheong, Y., 2018. In vivo oxygen, temperature and pH dynamics in the female reproductive tract and their importance in human conception: a systematic review. Hum. Reprod. Update 24 (1), 15–34.
Njagi, P., Groot, W., Arsenijevic, J., Dyer, S., Mburu, G., Kiarie, J., 2023. Financial costs of assisted reproductive technology for patients in low- and middle-income countries: a systematic review. Hum Reprod Open 2023 (2), hoad007.
Ortiz, A., Espino, J., Bejarano, I., Lozano, G.M., Monllor, F., García, J.F., Pariente, J.A., Rodríguez, A.B., 2011. High endogenous melatonin concentrations enhance sperm quality and short-term in vitro exposure to melatonin improves aspects of sperm motility. J. Pineal Res. 50 (2), 132–139.
Papis, K., Poleszczuk, O., Wenta-Muchalska, E., Modlinski, J.A., 2007. Melatonin effect on bovine embryo development in vitro in relation to oxygen concentration. J. Pineal Res. 43 (4), 321–326.
Qin, W., Guo, J., Gou, W., Wu, S., Guo, N., Zhao, Y., Hou, W., 2022. Molecular mechanisms of isoflavone puerarin against cardiovascular diseases: what we know and where we go. Chinese Herbal Medicines 14 (2), 234–243.
Reiter, R.J., Mayo, J.C., Tan, D.X., Sainz, R.M., Alatorre-Jimenez, M., Qin, L., 2016. Melatonin as an antioxidant: under promises but over delivers. J. Pineal Res. 61 (3), 253–278.
Richani, D., Dunning, K.R., Thompson, J.G., Gilchrist, R.B., 2021. Metabolic co-dependence of the oocyte and cumulus cells: essential role in determining oocyte developmental competence. Hum. Reprod. Update 27 (1), 27–47.
Rodriguez-Osorio, N., Kim, I.J., Wang, H., Kaya, A., Memili, E., 2007. Melatonin increases cleavage rate of porcine preimplantation embryos in vitro. J. Pineal Res. 43 (3), 283–288.
Sales, V.M., Ferguson-Smith, A.C., Patti, M.E., 2017. Epigenetic Mechanisms of Transmission of Metabolic Disease across Generations. Cell Metab. 25 (3), 559–571.
Shen, X., Sheng, H., Zhang, Y., Dong, X., Kou, L., Yao, Q., Zhao, X., 2024. Nanomedicine-based disulfiram and metal ion co-delivery strategies for cancer treatment. International Journal of Pharmaceutics: X 7, 100248.
Succu, S., Pasciu, V., Manca, M.E., Chelucci, S., Torres-Rovira, L., Leoni, G.G., Zinellu, A., Carru, C., Naitana, S., Berlinguer, F., 2014. Dose-dependent effect of melatonin on postwarming development of vitrified ovine embryos. Theriogenology 81 (8), 1058–1066.
Sugino, N., 2005. Reactive oxygen species in ovarian physiology. Reprod Med Biol 4 (1), 31–44.
Tai, B., Bai, L., Ji, R., Yu, M., Nala, L., Huang, H. Zheng, 2022. Phytochemical and pharmacological progress on Syringa oblata, a traditional Mongolian medicine. Chinese Herbal Medicines 14 (3), 392–402.
Telfer, E.E., Grosbois, J., Odey, Y.L., Rosario, R., Anderson, R.A., 2023. Making a good egg: human oocyte health, aging, and in vitro development. Physiol. Rev. 103 (4), 2623–2677.
von Mengden, L., Klamt, F., Smitz, J., 2020. Redox Biology of Human Cumulus Cells: Basic Concepts, Impact on Oocyte Quality, and potential Clinical Use. Antioxid. Redox Signal. 32 (8), 522–535.
Whitaker, M., 2006. Calcium at fertilization and in early development. Physiol. Rev. 86 (1), 25–88.
Xia, X., Sun, T., Zhao, Y., Sheng, H., Dong, X., Cheng, Y., Wu, F., Kou, L., Chen, R., Yao, Q., Zhang, H., 2024. Bilirubin Nanoparticles Alleviate Sepsis-Induced Acute Lung Injury by Protecting Pulmonary Endothelia Glycocalyx and reducing Inflammation. ACS Applied Nano Materials. https://doi.org/10.1021/acsanm.4c02015.
Xu, Y., Lv, L., Wang, Q., Yao, Q., Kou, L., Zhang, H., 2024. Emerging application of nanomedicine-based therapy in acute respiratory distress syndrome. Colloids Surf. B Biointerfaces 237, 113869.
Yao, Q., Jiang, X., Huang, Z.W., Lan, Q.H., Wang, L.F., Chen, R., Li, X.Z., Kou, L., Xu, H. L., Zhao, Y.Z., 2019a. Bilirubin Improves the Quality and Function of Hypothermic Preserved Islets by its Antioxidative and Anti-inflammatory effect. Transplantation 103 (12), 2486–2496.
Yao, Q., Jiang, X., Kou, L., Samuriwo, A.T., Xu, H.L., Zhao, Y.Z., 2019b. Pharmacological actions and therapeutic potentials of bilirubin in islet transplantation for the treatment of diabetes. Pharmacol. Res. 145, 104256.
Yao, Q., Huang, Z.W., Zhai, Y.Y., Yue, M., Luo, L.Z., Xue, P.P., Han, Y.H., Xu, H.L., Kou, L., Zhao, Y.Z., 2020a. Localized controlled release of bilirubin from beta-cyclodextrin-conjugated epsilon-polylysine to attenuate oxidative stress and inflammation in transplanted islets. ACS Appl. Mater. Interfaces 12 (5), 5462–5475.
Yao, Q., Lan, Q.H., Jiang, X., Du, C.C., Zhai, Y.Y., Shen, X., Xu, H.L., Xiao, J., Kou, L., Zhao, Y.Z., 2020b. Bioinspired biliverdin/silk fibroin hydrogel for antiglioma photothermal therapy and wound healing. Theranostics 10 (25), 11719–11736.
Yao, Q., Jiang, X., Zhai, Y.Y., Luo, L.Z., Xu, H.L., Xiao, J., Kou, L., Zhao, Y.Z., 2020c. Protective effects and mechanisms of bilirubin nanomedicine against acute pancreatitis. J. Control. Release 322, 312–325.
Yao, Q., Sun, R., Bao, S., Chen, R., Kou, L., 2020d. Bilirubin Protects Transplanted Islets by Targeting Ferroptosis. Front. Pharmacol. 11, 907.
Yao, Q., Chen, R., Ganapathy, V., Kou, L., 2020e. Therapeutic application and construction of bilirubin incorporated nanoparticles. J. Control. Release 328, 407–424.
Yao, Q., Shi, Y., Xia, X., Tang, Y., Jiang, X., Zheng, Y.W., Zhang, H., Chen, R., Kou, L., 2021. Bioadhesive hydrogel comprising bilirubin/beta-cyclodextrin inclusion complexes promote diabetic wound healing. Pharm. Biol. 59 (1), 1139–1149.
Yao, Q., Tang, Y., Dai, S., Huang, L., Jiang, Z., Zheng, S., Sun, M., Xu, Y., Lu, R., Sun, T., Huang, H., Jiang, X., Yao, X., Lin, G., Kou, L., Chen, R., 2023a. A Biomimetic Nanoparticle Exerting Protection against Acute Liver failure by Suppressing CYP2E1 activity and Scavenging Excessive ROS. Adv. Healthc. Mater. 12 (24), e2300571.
Yao, Q., Zhai, Y.-Y., He, Z., Wang, Q., Sun, L., Sun, T., Lv, L., Li, Y., Yang, J., Lv, D., Chen, R., Zhang, H., Luo, X., Kou, L., 2023b. Water-responsive gel extends drug retention and facilitates skin penetration for curcumin topical delivery against psoriasis. Asian Journal of Pharmaceutical Sciences 100782.
Yao, Q., Ye, J., Chen, Y., Huang, L., Sun, L., He, Z., Wu, J., Zhao, Y., Zhao, X., Cai, A., Chen, X., Zheng, H., Sysa, A., Xie, C., Chen, R., Kou, L., 2024. Modulation of glucose metabolism through macrophage-membrane-coated metal-organic framework nanoparticles for triple-negative breast cancer therapy. Chem. Eng. J. 480, 148069.
Zhao, Y.Z., Huang, Z.W., Zhai, Y.Y., Shi, Y., Du, C.C., Zhai, J., Xu, H.L., Xiao, J., Kou, L., Yao, Q., 2021. Polylysine-bilirubin conjugates maintain functional islets and promote M2 macrophage polarization. Acta Biomater. 122, 172–185.
Zhao, X., Duan, B., Wu, J., Huang, L., Dai, S., Ding, J., Sun, M., Lin, X., Jiang, Y., Sun, T., Lu, R., Huang, H., Lin, G., Chen, R., Yao, Q., Kou, L., 2024. Bilirubin ameliorates osteoarthritis via activating Nrf2/HO-1 pathway and suppressing NF-kappaB signalling. J. Cell. Mol. Med. 28 (7), e18173.